

EXPERIMENTAL INVESTIGATION ON THE INFLUENCE OF LATERAL EARTH PRESSURES ON RETAINING WALLS

¹Tan, J.H., ¹Karunakaran, P.*

¹Centre of Advances Engineering Design, Faculty of Engineering, Built Environment and Information Technology, SEGI University, 47810 Petaling Jaya, Selangor, Malaysia.

*Corresponding Author: priyadatchinikarunkaran@segi.edu.my TEL: (603)-61451777

Received: 13 June 2024; Accepted: 05 July 2024; Published: 31 December 2024

doi: 10.35934/segi.v10i2.106

Highlights:

- Retaining wall failures are common in tropical regions like Malaysia.
- The study analyzing lateral earth pressure and its impact on retaining wall resilience.
- Research utilizes prototypes to examine failure mechanisms in L-shaped cantilever walls.
- Findings show that higher water tables reduce safety factors and increase wall deformation.

Abstract: Despite continual advancement in retaining wall technology, failures of these structures still frequently make national news. In tropical countries like Malaysia, rainfall-induced landslides are a primary cause of these failures. Bridging the gaps in the Sustainable Development Goals (SDGs) of Sustainable Cities and Communities (SDG11), this study offers valuable insights to the importance of lateral earth pressure and its effects on retaining walls, therefore fostering the development of resilient infrastructure for the future. By focusing on prototype development and software simulations, this study investigates the failure mechanisms of an L-shaped cantilever retaining wall influenced by different groundwater table profiles, with a constant surcharge atop the backfill soil. The results indicate that the higher water tables correlate with lower factor of safety (FOS) and increased wall deformation. The results obtained using both software and prototype modelling shows FOS of sliding, overturning, and bearing capacity failure did not satisfy the requirement set by authorities due to the overloading and insufficient design of the geometry of the wall. These findings provide practical implications and are consistent with existing literature. Thus, this study provides an easy yet solid methodology to research on lateral earth pressures for future endeavours.

Keywords: prototype development; retaining wall; SDGs; software simulation; wall stability

1. Introduction

Landslides are common natural phenomenon on our planet (Wang, 2023). They are characterised by the rapid movement of earth, rocks, or debris down a slope under the influence of gravity (Sharma *et al.*, 2023). To mitigate landslides, retaining walls, such as cantilever walls, gravity walls, and counterfort walls, are often constructed. These walls retain soil on one side, preventing it from sliding down slopes (Binici *et al.*, 2010; Chikute & Sonar, 2019; Koopialipoor *et al.*, 2020).

Kong *et al.* (2021) provided insights into the various types of retaining wall failures, as illustrated in **Figure 1**. Although retaining walls have successfully mitigated landslides, they remain susceptible to deformation and failure due to complex soil parameters, fluctuating porewater pressure, increasing surcharge loads, and inaccurate slope angles (Yoo *et al.*, 2006; Cao *et al.*, 2016; Chikute & Sonar, 2019; Liu, 2019).

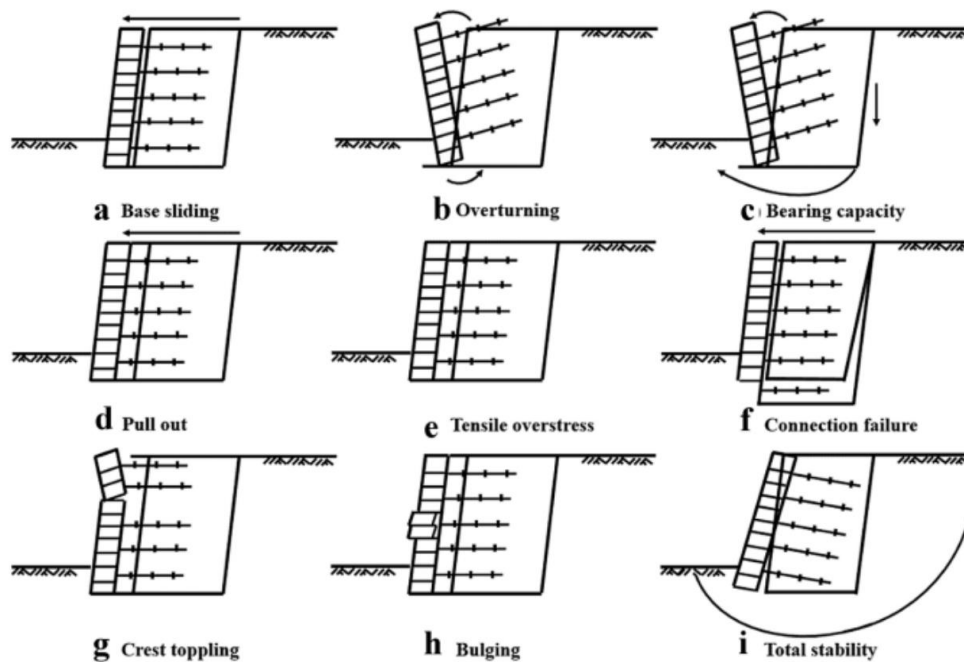


Figure 1. Types of retaining wall failures (Kong *et al.*, 2021)

Malaysia's tropical climate exacerbates these issues, as soil shrinkage and swelling, coupled with blocked drainage, frequently compromise the integrity of retaining walls (Dorairaj & Osman, 2021). The primary cause of retaining wall failure is the earth pressure exerted on the wall's surface. Koopialipoor *et al.* (2020) emphasized that accurately determining the lateral earth pressure behind the wall is critical for designing and ensuring the stability of retaining walls. Since lateral forces

arise from the physical properties of the backfill soil, porewater pressure within the backfill, and any surcharge applied on top of the backfill, a comprehensive understanding of lateral earth pressures is essential. Additionally, GL *et al.* (2016) noted that most retaining wall failures result from errors in the design of the backfill.

Sharma & Baradiya (2014) identified lateral earth pressure as the primary force impacting a retaining wall, which seeks to deflect, slide, and potentially overturn the structure. The magnitude and direction of this pressure are determined based on soil mechanics principles. Cernica (1995) stated that lateral earth pressure depends on five factors: (1) the physical attributes of the soil; (2) the time-dependent behavior of soil strength; (3) the interaction between the soil and the retaining structure at their interface; (4) the overall deformation characteristics of the soil-structure composite; and (5) the applied loading, such as the height of backfill, slope gradient, and surcharge loads. The author further indicated that the earth pressure value is constrained within upper and lower limits.

Perozzi & Puzrin (2023) explained that the lower limit of the earth pressure is determined by the active earth pressure, which occurs when the retaining wall moves away from the soil mass. Conversely, the upper limit is established by the passive earth pressure, which arises when the wall moves towards the soil mass. The active force, P_a and passive force, P_p per unit length of the retaining wall is denoted as:

$$P_a = \frac{1}{2} \gamma H^2 K_a \quad (1)$$

$$P_p = \frac{1}{2} \gamma H^2 K_p \quad (2)$$

where γ is the unit weight of the earth (kN/m^3), H is the height of the retaining wall (m), and K is the coefficient that relies on the physical properties of the retained soil, and on whether the pressure is active, K_a or passive, K_p (Hooley & Al-Deen, 2020).

Below are the equations to obtain the active and passive coefficient for the force per unit length acting on the retaining wall (Das, 2011):

$$K_a = \frac{1 - \sin\phi}{1 + \sin\phi} \quad (3)$$

$$K_p = \frac{1 + \sin\phi}{1 - \sin\phi} \quad (4)$$

where ϕ is the angle of shearing resistance of the retained soil.

When the backfill of the retaining wall has a slope, the equation of K_a and K_p should be changed as follows (Perozzi & Puzrin, 2023):

$$K_a = \frac{\cos\phi - \sqrt{\cos^2\theta - \cos^2\phi}}{\cos\phi + \sqrt{\cos^2\theta - \cos^2\phi}} \cos\phi \quad (5)$$

$$K_p = \frac{\cos\phi + \sqrt{\cos^2\theta - \cos^2\phi}}{\cos\phi - \sqrt{\cos^2\theta - \cos^2\phi}} \cos\phi \quad (6)$$

where θ is the inclined angle of the slope with respect to the horizontal. As shown in equation (1) and (2), the unit weight of the retained soil plays a very crucial parameter in the equation as it will affect the overall outcome of the lateral stress acting on the wall. With the introduction of water, the lateral forces exerted on the wall due to porewater pressure, u , must be considered.

One of the infamous tragedies that involved with retaining wall failures that happened in Malaysia was the Highland Tower collapse in Taman Hillview, Ulu Klang, Selangor, Malaysia on the 11th December 1993. The Highland Tower condominiums consist of three building blocks, which are block 1, 2, and 3. After ten consecutive days of rainfall in the area, Block 1 of the three building blocks collapsed, causing 48 losses of lives, including children. One of the main factors that lead to this tragedy was the poor drainage system of the retaining walls that could not keep up with the infiltration rate of the surface runoff during the rain (Azuwa & Yahaya, 2023). This leads to the porewater buildup behind the retaining wall, hence increasing the lateral earth pressure, and finally causing it to collapse.

In recent years, there has been a considerable emphasis on integrating advanced tools and analytical methods to develop innovative technologies in civil engineering. Despite these advancements, retaining wall failures remains a persistent issue, frequently making national headlines and underscoring the need for further research and education in this field. Reports from various newspapers often document such failures, highlighting the urgency of addressing this problem (Wahab, 2022; Bernama, 2023; Anthony & Ng, 2023). According to Karunakaran *et al.* (2018), unaddressed issues or delay in decision making led to project cost overruns.

Based on the Department of Information Malaysia (2016), the annual rainfall is 80% a year which contributes between 2000 mm to 2500 mm of precipitation. Understanding the stability and behavior of retaining walls under different water table profiles is fundamental for beginners, and

this can be achieved through practical approaches such as prototype development and software simulation. By adopting these methods, gaps in the Sustainable Development Goals (SDGs), particularly Sustainable Cities and Communities (SDG 11), can be minimized.

Therefore, this study aims to enhance the understanding of lateral earth pressure and its effects on retaining walls by focusing on prototype development and software simulations. This approach contributes to achieving SDG 11 and paves the way for developing resilient infrastructure capable of withstanding the challenges posed by tropical climates and intense rainfall. In alignment with the study's aim, this study focuses on investigating the stability of an L-shaped cantilever retaining wall influenced by various water table profiles, with a constant surcharge atop the backfill soil. This study can provide insights into the failure mechanisms of such structures and propose potential solutions.

2. Methodology

The methodology of this study involves three parts. The first is on the prototype development, the second is experimenting the wall failure based on different water table profiles, and the third is to assess the integrity of the wall as well as to evaluate the factor of safety of the backfill mass retained by the wall.

2.1. Prototype Development

The apparatus and materials used in this development together with the experimental setup is discussed in detail in the following sections.

2.1.1. Transparent Apparatus

The transparent apparatus, depicted in **Figure 2(a)**, serves as a container to hold the soil sample, water, and the cantilever wall in place. The dimension of the apparatus was 29 cm × 18 cm × 26 cm. A glass aquarium was chosen for this experiment due to its smooth and transparent surface, which minimises friction between the soil sample and the surface of the aquarium. Additionally, the transparency allows for clear observation of the experiment's outcome. To ensure consistency in the experimental setup, markings indicating the position of the cantilever wall and the height of the foundation soil were made on the aquarium. These markings serve as the original coordinates of the cantilever wall before any pressures are applied to the backfill. By using these coordinates as a reference, the deformation of the wall can be observed and measured accurately.

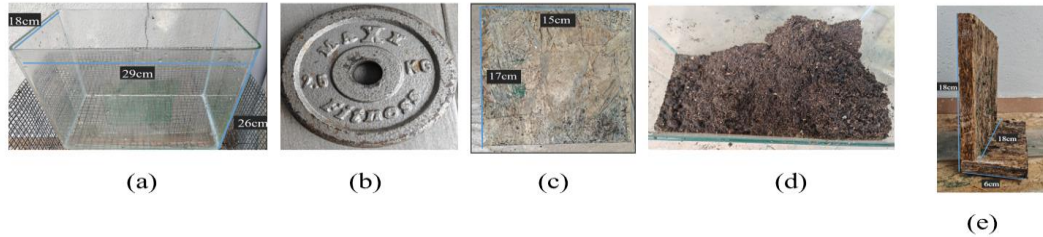


Figure 2. (a) An transparent apparatus to hold the experiment together, (b) 2.5kg metal plate, (c) 17 cm × 15 cm plank to ensure uniform loading, (d) soil sample, and (e) wooden L-shaped cantilever wall

2.1.2. Surcharge

Figure 2(b) shows the metal plates used to provide a constant load on top of the backfill. Each plate has a mass of 2.5kg. Two plates are used during the experiment, which represents a surcharge load of 2 kPa. The metal plates are placed on top of a rectangular board with a dimension of 17 cm × 15 cm, as shown in **Figure 2(c)**. This setup ensures a uniform load of 2 kPa across the area of the backfill soil.

2.1.3. Soil Sample

The soil sample used in this experiment is shown in **Figure 2(d)**. A 4cm layer of soil was laid as a foundation soil at the bottom of the aquarium, with dimensions of 17 cm × 15 cm × 18 cm. The soil sample is marine clay that was obtained from Bandar Sulaiman, Klang, and its properties are readily available in SEGI laboratory. The specific soil parameters are listed in **Table 1**.

Table 1. Specific soil parameters used in this study

Soil parameters	Data
Optimum Moisture Content, OMC	20.24 kN/m ³
Maximum Dry Density, MDD	8.77%
Specific Gravity, G _s	2.17
Shrinkage Limit	26.31%
Liquid Limit, LL	19.23%
Plastic Limit, PL	7.08%
Plastic Index, PI	7.30%
Bulk Density, <i>Y</i>	15 kN/m ³

2.1.4. Water Content

To investigate the impact of varying water content on the backfill material, different percentages of water (0%, 20%, 40%, 60%, 80%, and 100%) were mixed with a backfill sample having a constant volume of 4950cm³. The corresponding volumes of water added is shown in **Table 2**:

Table 2. Percentage of water with the corresponding volumes of water added

Percentage of water (%)	Corresponding volumes of water added (L)
0	0
20	1
40	2
60	3
80	4
100	5

Each water content percentage was thoroughly mixed with the backfill to ensure even distribution throughout the sample.

2.1.5. Wooden L-shaped Cantilever Retaining Wall

A wooden L-shaped cantilever retaining wall model, depicted in **Figure 2(e)**, was handcrafted from 1 cm thick fibreboard. The model measures 18 cm in height, 18 cm in width, and 6 cm in depth. The construction involved using two separate fibreboards, which were joined using three nails and reinforced with super glue to ensure additional stability. This model was created to simulate the behaviour of cantilever wall, forming a crucial part of the experimental setup for investigating the influence of varying water content on the backfill material.

2.2. Experimental Set-up

The first step is the soil sample were dried using natural sunlight until completely devoid of moisture, ensuring removal of any water content present. This step is crucial to establish the baseline condition for subsequent manipulation of the soil's water content to align with the experimental objectives. To ensure reproducibility, the second step is original coordinates are marked for precise model reconstruction. Following complete drying of the soil sample, a 4 cm foundation layer is meticulously laid and levelled beneath the aquarium base. Subsequently, a wooden L-shaped cantilever wall is positioned 17 cm from the right. Step three, the methodology

involves filling dried soil samples alongside a cantilever wall positioned on a hillside. The soil is incrementally added until it reaches the same height as the cantilever wall. This process ensures that the soil level matches the wall's height, providing a stable foundation and accurately simulating real-world conditions. The fourth step is to apply a uniform surcharge to the backfill, a rectangular wooden plank measuring 18 cm × 17 cm is utilised. Onto this plank, two weight plates with a combined mass of 2.5kg are positioned centred, resulting in a uniform surcharge of 2 kPa. Lastly, the setup was left undisturbed for 30 minutes to ensure the wall has reached maximum displacement. The overall step of the experimental setup is illustrated in **Figure 3**.



Figure 3. Experimental setup

2.3. Software Analysis

2.3.1. Wall Stability Analysis

Tekla Tedds (Trimble, 2021) was utilized to calculate the factor of safety (FOS) of the external stability of the cantilever wall. Tekla Tedds retaining wall design offers an easy retaining wall design, with quick and precise structural and civil calculations. It can replace time-consuming manual calculations and spreadsheets, hence saving precious time and increasing work efficiency. Tekla Tedds provides superb libraries. It eliminates mistakes and speeds up code-compliant design output by utilizing a quality-assured database of frequently updated multi-material computations. Additionally, Tedds provides straightforward computations. The computations are clearly apparent, allowing for easy examination and verification. Additionally, it provides expert documentation. Designers may use desktop publishing technologies to swiftly produce and adjust data production for professional, consistent documentation of projects.

The original dimension of the wall is given as follows:

- Retained soil height = 18 cm (180 mm)
- Stem height = 18 cm (180 mm)
- thickness = 1.5 cm (15 mm)
- Heel length = 6 cm (60 mm)

For the software simulation, a factor of 10 is multiplied to the original dimensions of the wall to allow the software to simulate the problem. The following is the factorised dimensions applied:

- Retained soil height = 180 cm (1800 mm)
- Stem height = 180 cm (1800 mm)
- thickness = 15 cm (150 mm)
- Heel length = 60 cm (600 mm)

The height of the water table is set to 0 mm, 360 mm, 720 mm, 1080 mm, 1440 mm, and 1800 mm for 0%, 20%, 40%, 60%, 80%, and 100% water content, respectively. The report of the analysis is then generated.

2.3.2. Slope Stability Analysis

Slope/W (GeoStudio, 2021) is a limit equilibrium slope stability software developed by GeoStudio for calculating factors of safety, slip surface, porewater pressures, and analytical calculations of slopes. The software is used to calculate the global stability of unreinforced and reinforced slope under varying water content in the backfill soil while a constant surcharge is acting upon it.

In Slope/W, water table is defined using a piezometric line which is drawn across the region of the slope. In this study, various water tables are defined according to different water content of the slope. **Figure 4** shows the slope with a 20% water content water table. **Table 3** shows the relationship between the height of the water table and the water content of the slope.

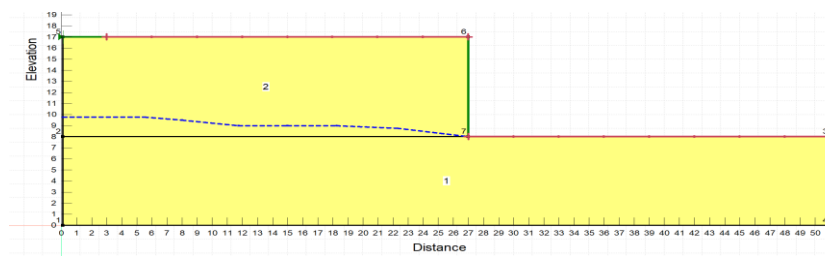


Figure 4. Slope with a 20% water content water table

Table 3. Relationship between the height of the water table and the water content of the slope

No	Water Content (%)	Height of Water Table (m)
1	0	0
2	20	1.8
3	40	3.6
4	60	5.4
5	80	7.2
6	100	9.0

3. Results and Discussion

3.1. Experimental Results

Following the completion of the experimental setup, a predetermined proportion of water relative to the total volume of the retained soil as shown in **Table 4** is introduced into the soil sample. Subsequent placement of the surcharge atop the retained soil initiates wall deformation. By marking the original position of the wall on the aquarium surface as shown in **Figure 3**, the displacement of the wooden L-shaped cantilever wall becomes perceptible. The apparatus remains undisturbed for one hour to allow maximal deformation. Recorded outcomes are documented, as delineated in **Table 4**. **Figure 5** illustrates the wall deformation across varied water content levels in the backfill soil throughout the experiment.

Table 4. The outcome of the experiment

Percentage of Water Added (%)	Volume of Water Added in Liters (L)	Sliding	Bearing capacity	Overturning
		Lateral Displacement (mm)	Settlement (mm)	Inclination (°)
0	0	3	8	7
20	1	3	8	7
40	2	11	11	6
60	3	13	15	11
80	4	20	18.5	12
100	5	22	18.5	15

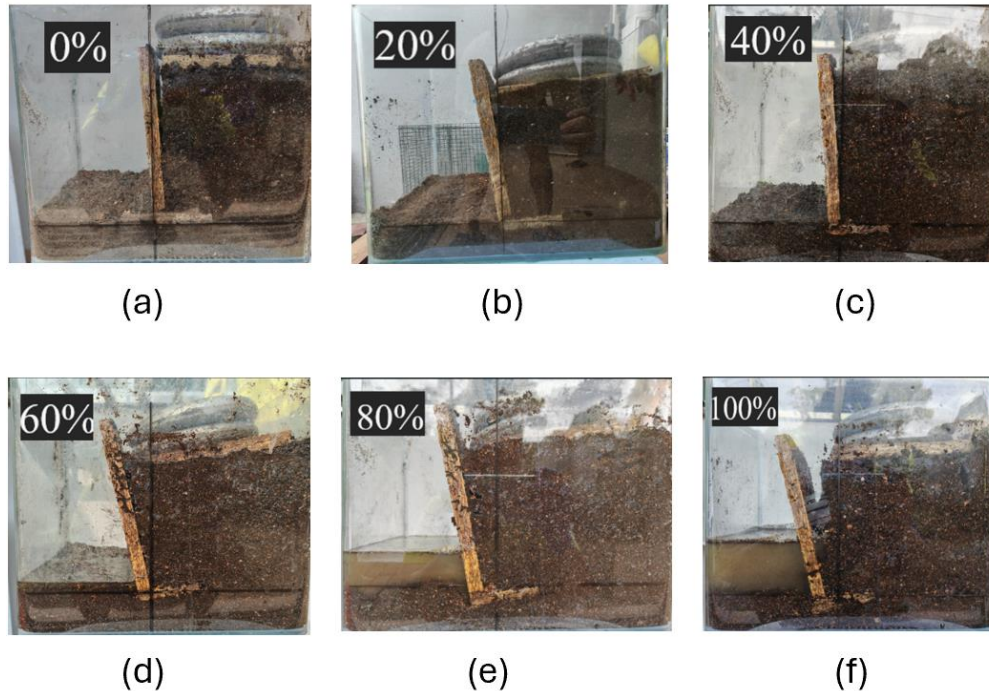


Figure 5. Incremental of water content in percentages

Based on the findings, it is evident that the deformation of the cantilever wall exacerbates with increased water content introduced into the backfill soil. This phenomenon finds explanation through the theories of lateral earth pressure elucidated.

3.2. Tekla Tedd Analysis Results

Tekla Tedds was used to simulate the external stability of the wooden L-shaped cantilever wall in terms of its factor of safety (FOS). With the results obtained in Tedds as shown in **Table 5**, further confirmation can be done to support the outcome obtained from the experiment above. As depicted in **Table 5**, the wall exhibits an inherent propensity for failure from the outset of the experiment, commencing at 0% water content in the backfill. Notably, the factor of safety (FOS) pertaining to both overturning and sliding stability diminishes progressively with escalating water table levels. Remarkably, the foundation soil's bearing pressure remains consistently null throughout the experimental duration. This discrepancy may stem from the utilization of a reinforced concrete cantilever wall in the software simulation, lacking a wooden counterpart. Given the former's substantially greater mass, the software predicts an inevitable failure of the foundation soil. Thus, synthesis of outcomes from both the prototype experiment and software simulation supports the inference that heightened water content in the backfill soil corresponds to elevated lateral earth

pressure, diminished FOS against sliding, overturning, and bearing capacity, ultimately resulting in augmented wall deformation.

Table 5. Results of the analysis of different water content

Water content (%)	Results	Water content (%)	Results																																
0	<table border="1"> <thead> <tr> <th></th> <th>Capacity</th> <th>Applied</th> <th>F o S</th> </tr> </thead> <tbody> <tr> <td>Sliding stability</td> <td>kN/m 8.4</td> <td>41.2</td> <td>0.203 ❌</td> </tr> <tr> <td>Overturning stability</td> <td>kNm/m 8.6</td> <td>28.4</td> <td>0.292 ❌</td> </tr> <tr> <td>Bearing pressure</td> <td>kN/m² 0</td> <td>0</td> <td>0.000 ❌</td> </tr> </tbody> </table> <p>FAIL - Reaction acts outside base area! ❌</p>		Capacity	Applied	F o S	Sliding stability	kN/m 8.4	41.2	0.203 ❌	Overturning stability	kNm/m 8.6	28.4	0.292 ❌	Bearing pressure	kN/m ² 0	0	0.000 ❌	60	<table border="1"> <thead> <tr> <th></th> <th>Capacity</th> <th>Applied</th> <th>F o S</th> </tr> </thead> <tbody> <tr> <td>Sliding stability</td> <td>kN/m 7</td> <td>41.4</td> <td>0.168 ❌</td> </tr> <tr> <td>Overturning stability</td> <td>kNm/m 8.6</td> <td>30.8</td> <td>0.278 ❌</td> </tr> <tr> <td>Bearing pressure</td> <td>kN/m² 0</td> <td>0</td> <td>0.000 ❌</td> </tr> </tbody> </table> <p>FAIL - Reaction acts outside base area! ❌</p>		Capacity	Applied	F o S	Sliding stability	kN/m 7	41.4	0.168 ❌	Overturning stability	kNm/m 8.6	30.8	0.278 ❌	Bearing pressure	kN/m ² 0	0	0.000 ❌
	Capacity	Applied	F o S																																
Sliding stability	kN/m 8.4	41.2	0.203 ❌																																
Overturning stability	kNm/m 8.6	28.4	0.292 ❌																																
Bearing pressure	kN/m ² 0	0	0.000 ❌																																
	Capacity	Applied	F o S																																
Sliding stability	kN/m 7	41.4	0.168 ❌																																
Overturning stability	kNm/m 8.6	30.8	0.278 ❌																																
Bearing pressure	kN/m ² 0	0	0.000 ❌																																
20	<table border="1"> <thead> <tr> <th></th> <th>Capacity</th> <th>Applied</th> <th>F o S</th> </tr> </thead> <tbody> <tr> <td>Sliding stability</td> <td>kN/m 7.8</td> <td>41.2</td> <td>0.189 ❌</td> </tr> <tr> <td>Overturning stability</td> <td>kNm/m 8.6</td> <td>29.4</td> <td>0.292 ❌</td> </tr> <tr> <td>Bearing pressure</td> <td>kN/m² 0</td> <td>0</td> <td>0.000 ❌</td> </tr> </tbody> </table> <p>FAIL - Reaction acts outside base area! ❌</p>		Capacity	Applied	F o S	Sliding stability	kN/m 7.8	41.2	0.189 ❌	Overturning stability	kNm/m 8.6	29.4	0.292 ❌	Bearing pressure	kN/m ² 0	0	0.000 ❌	80	<table border="1"> <thead> <tr> <th></th> <th>Capacity</th> <th>Applied</th> <th>F o S</th> </tr> </thead> <tbody> <tr> <td>Sliding stability</td> <td>kN/m 6.5</td> <td>41.6</td> <td>0.157 ❌</td> </tr> <tr> <td>Overturning stability</td> <td>kNm/m 8.6</td> <td>31.6</td> <td>0.271 ❌</td> </tr> <tr> <td>Bearing pressure</td> <td>kN/m² 0</td> <td>0</td> <td>0.000 ❌</td> </tr> </tbody> </table> <p>FAIL - Reaction acts outside base area! ❌</p>		Capacity	Applied	F o S	Sliding stability	kN/m 6.5	41.6	0.157 ❌	Overturning stability	kNm/m 8.6	31.6	0.271 ❌	Bearing pressure	kN/m ² 0	0	0.000 ❌
	Capacity	Applied	F o S																																
Sliding stability	kN/m 7.8	41.2	0.189 ❌																																
Overturning stability	kNm/m 8.6	29.4	0.292 ❌																																
Bearing pressure	kN/m ² 0	0	0.000 ❌																																
	Capacity	Applied	F o S																																
Sliding stability	kN/m 6.5	41.6	0.157 ❌																																
Overturning stability	kNm/m 8.6	31.6	0.271 ❌																																
Bearing pressure	kN/m ² 0	0	0.000 ❌																																
40	<table border="1"> <thead> <tr> <th></th> <th>Capacity</th> <th>Applied</th> <th>F o S</th> </tr> </thead> <tbody> <tr> <td>Sliding stability</td> <td>kN/m 7.4</td> <td>41.3</td> <td>0.178 ❌</td> </tr> <tr> <td>Overturning stability</td> <td>kNm/m 8.6</td> <td>30.1</td> <td>0.285 ❌</td> </tr> <tr> <td>Bearing pressure</td> <td>kN/m² 0</td> <td>0</td> <td>0.000 ❌</td> </tr> </tbody> </table> <p>FAIL - Reaction acts outside base area! ❌</p>		Capacity	Applied	F o S	Sliding stability	kN/m 7.4	41.3	0.178 ❌	Overturning stability	kNm/m 8.6	30.1	0.285 ❌	Bearing pressure	kN/m ² 0	0	0.000 ❌	100	<table border="1"> <thead> <tr> <th></th> <th>Capacity</th> <th>Applied</th> <th>F o S</th> </tr> </thead> <tbody> <tr> <td>Sliding stability</td> <td>kN/m 6.1</td> <td>41.8</td> <td>0.146 ❌</td> </tr> <tr> <td>Overturning stability</td> <td>kNm/m 8.6</td> <td>32.4</td> <td>0.264 ❌</td> </tr> <tr> <td>Bearing pressure</td> <td>kN/m² 0</td> <td>0</td> <td>0.000 ❌</td> </tr> </tbody> </table> <p>FAIL - Reaction acts outside base area! ❌</p>		Capacity	Applied	F o S	Sliding stability	kN/m 6.1	41.8	0.146 ❌	Overturning stability	kNm/m 8.6	32.4	0.264 ❌	Bearing pressure	kN/m ² 0	0	0.000 ❌
	Capacity	Applied	F o S																																
Sliding stability	kN/m 7.4	41.3	0.178 ❌																																
Overturning stability	kNm/m 8.6	30.1	0.285 ❌																																
Bearing pressure	kN/m ² 0	0	0.000 ❌																																
	Capacity	Applied	F o S																																
Sliding stability	kN/m 6.1	41.8	0.146 ❌																																
Overturning stability	kNm/m 8.6	32.4	0.264 ❌																																
Bearing pressure	kN/m ² 0	0	0.000 ❌																																

3.3. Slope/W Analysis Results

Table 6 and Table 7 offer a succinct overview of the factor of safety (FOS) pertaining to the unreinforced and reinforced slopes, respectively.

Table 6. FOS of unreinforced slope with respect to different height of water table

No.	Water Content (%)	Height of Water Table (m)	FOS
1	0	0	1.215
2	20	1.8	1.186
3	40	3.6	1.150
4	60	5.4	1.089
5	80	7.2	1.044
6	100	9.0	0.957

The FOS of the unreinforced slope based by the slope guidelines set by Slope Engineering Branch, JKR (2010) is at least 1.3. However, all the cases simulated in the software as shown in Table 6

had not met the requirement of FOS 1.3 from the start of the simulation. Therefore, the slope is deemed to be unsafe with the combination of geometry and the soil type.

Table 7. FOS of reinforced slope with respect to different height of water table

No.	Water Content (%)	Height of Water Table (m)	FOS
1	0	0	1.328
2	20	1.8	1.327
3	40	3.6	1.310
4	60	5.4	1.301
5	80	7.2	1.295
6	100	9.0	1.288

Based on the guidelines set by Slope Engineering Branch, JKR (2010), the FOS of a reinforced slope should be more than 1.5. Nevertheless, the results in **Table 7** shows that the FOS of the reinforced slopes are all less than the requirement. In short, the slope still fails after the L-shaped cantilever wall is used as a remedial method.

The results from both reinforced and unreinforced slope show a decrease in FOS when the water table increases. This can be explained using the lateral forces theory. The higher the pore-water pressure in the slope or backfill, the higher the lateral forces acting on the retaining wall. This will destabilize the wall, hence reducing the FOS of the wall in terms of global stability.

3.4. Comparison of Results

The outcomes derived from prototype experiment, Tekla Tedds, and Slope/W are compared to analyses the similarities and differences between them. **Table 8** shows comparison between the three sets of data.

Following the addition of water and surcharge to the backfill soil, a protractor measures the wall's inclination angle, directly linked to its propensity for overturning. As porewater pressure increases, so does lateral earth pressure, augmenting the wall's overturning moment ($\sum M_o$) (kNm) (Perozzi & Puzrin, 2023). With the increase of ($\sum M_o$), the FOS decreases according to the equation $F. O. S = \frac{\sum M_R}{\sum M_o}$, where $\sum M_R$ is the resisting moment in kNm (Ranjbar Karkanaki *et al.*, 2017). Heightened overturning moments diminish the factor of safety (FOS) against overturning, as seen in **Table 8**, where the degree of inclination rises with water content. The use of a lighter material, such as a

wooden L-shaped cantilever wall in this experiment, reduces the resisting overturning moment compared to reinforced concrete.

Table 8. Comparison of data

Deformation of Experimental				Software (FOS)				
Prototype				Tekla Tedds			Slope/W	
Water Content (%)	Sliding (mm)	Settlement (mm)	Overturning (°)	Sliding	Settlement	Overturning	Global Stability	
							Unreinforced	Reinforced
0	3	8	7	0.203	0	0.302	1.215	1.328
20	3	8	7	0.189	0	0.292	1.186	1.327
40	11	11	6	0.178	0	0.285	1.150	1.310
60	13	15	11	0.168	0	0.278	1.089	1.301
80	20	18.5	12	0.157	0	0.271	1.044	1.295
100	22	18.5	15	0.146	0	0.264	0.957	1.288

Assessing sliding involves measuring lateral displacement after water and surcharge introduction. Vertical force ($\sum H$) (kN) from the backfill escalates with water, reducing FOS against sliding $F.O.S = \frac{\mu \sum W}{\sum H}$, where $\sum W$ is the total of vertical forces in kN (Sharma & Baradiya, 2014). The calculation incorporates the friction coefficient (μ) between the wall and soil (Cernica, 1995). Real-life deviations may occur due to wood usage instead of reinforced concrete.

Bearing capacity failure assessment measures post-experiment wall settlement. The equation $F.O.S = \frac{\sigma_f \times B'}{R_v}$ accounts for the foundation soil's bearing capacity σ_f (kN/m³), impacting settlement resistance, where B' (m) is the length of the toe to the retaining wall, and R_v (kN) is the vertical component of the resultant force (Perozzi & Puzrin, 2023). Higher bearing capacity leads to reduced settlement. Marine clay, akin to the backfill, swells when in contact with water, decreasing its bearing capacity. Settlement stabilizes at 80% water content, reflecting maximum saturation and weakened strength.

4. Conclusion

In this endeavour, the impact of lateral earth pressures on retaining walls were investigated. Firstly, the factor of safety of unreinforced and reinforced soil was determined using software modelling such as Tekla Tedds and Slope/W for external stability and global stability respectively. Secondly, the deformation of retaining walls under various water pressures within the backfill using an

experimental prototype model was shown. Lastly, the outcome of both software and experimental studies were compared. From the results obtained from the whole study, the following conclusions can be drawn:

1. The higher the water table, the higher the porewater pressure within the backfill, the lower the FOS of the external and global stability of the retaining wall.
2. The higher the porewater pressure in the backfill, the higher the deformation of the retaining wall in terms of lateral displacement (sliding), settlement (bearing capacity failure), and overturning.
3. The importance of the adequate design of backfill and drainage system were highlighted to prevent the accumulation of porewater pressure in the backfill soil, hence preventing lateral earth pressure build up.
4. In research done by Du & Chen (2007) proves that the addition of shear keys in retaining walls can increase the FOS of the wall by 22%. Therefore, the geometry of the retaining wall such as shear keys, length of the toe and hill, and height of the stem of the retaining wall must be properly designed to improve the performance of the retaining wall.

This research aligns with SDG 11 Sustainable Cities and Communities respectively, as this research provides an easier way to understand the basic yet important geotechnical knowledge regarding lateral earth pressures and retaining wall failures through the development of the physical prototype and software simulations. Furthermore, with the knowledge on how retaining wall fails, future engineers can have better designs and solutions to this geotechnical problem that are more efficient and sustainable to the environment. This study serves as a foundation for future endeavours further into the topic with improvements such as reducing human errors and setting up more realistic soil and ground water table profiles.

Acknowledgement

The authors would like to thank SEGi University for supporting the research of this study.

Credit Author Statement

Conceptualization and methodology, Tan, J.H.; software and validation, Tan, J.H.; writing - original draft preparation, Tan, J.H.; writing - review and editing, Tan, J.H. and Karunakaran, P.; supervision and project administration, Karunakaran, P.

Conflicts of Interest

The authors declare no conflict of interest.

References

- Anthony, L., & Ng, K.C. (2023, June 23). Serious attention needed to prevent retaining wall failures (again). *Edge Drop News*. <https://www.edgeprop.my/content/1906454/serious-attention-needed-prevent-retaining-wall-failures-again>
- Azuwa, S.B., & Yahaya, F.B.M. (2023). Case study of block 1, Highland Towers condominium collapsed in Taman Hillview, Ulu Klang, Selangor, Malaysia on 11th December 1993. *Alexandria Engineering Journal*, 85, 86-103.
- Bernama. (2023, May 4). Collapsed Wisma YPR retaining wall occurred at privately owned premises. *New Straits Times*. <https://www.nst.com.my/news/nation/2023/05/905649/collapsed-wisma-ypr-retaining-wall-occurred-privately-owned-premises>
- Bıncı, H., Temiz, H., Kayadelen, C., Kaplan, H., & Durgun, M.Y. (2010). Retaining Wall failure due to poor construction and design aspects a case study. *Yapı Teknolojileri Elektronik Dergisi*, 6(1), 46-61.
- Cao, L., Peaker, S., & Ahmad, S. (2016). A case study of embankment retaining wall in Ontario. *In Proceedings of the 69th Canadian Geotechnical Conference—GeoVancouver*.
- Cernica, J.N. (1995). *Geotechnical Engineering: Soil Mechanics*. <http://pascal-francis.inist.fr/vibad/index.php?action=getRecordDetail&idt=6341729>
- Chikute, G.C., & Sonar, I.P. (2019). Failures of gabion walls. *International Journal of Innovative Technology and Exploring Engineering (IJITEE)*, 8(11), 1384-1390.
- Das, B.M. (Ed.). (2011). *Geotechnical engineering handbook*. J. Ross publishing.
- Department of Information, Malaysia. (2016). *Malaysia information*. <https://www.malaysia.gov.my/portal/content/144>
- Dorairaj, D., & Osman, N. (2021). Present practices and emerging opportunities in bioengineering for slope stabilization in Malaysia: An overview. *PeerJ*, 9, e10477.
- Du, C., & Chen, J. (2007). Numerical study of the effect of shear keys on the stability of cantilever retaining walls. *Sci-En-Tech. Com*.
- GeoStudio. (2021). Stability modelling with GEOSTUDIO. Stability modelling with SLOPE/W. <https://downloads.geoslope.com/geostudioresources/books/11/2/SLOPE%20Modeling.pdf>

- GL, S.B., Raja, P., & Rao, P.R. (2016). Forensic analysis of failure of retaining wall. *Japanese Geotechnical Society Special Publication*, 2(73), 2514-2519.
- Hooley, I.W., & Al-Deen, S. (2020). Design of cantilever retaining walls for minimum tilting tendency. *Australian Journal of Structural Engineering*, 21(3), 254-262.
- Karunakaran, P., Abdullah, A.H., Nagapan, S., Sohu, S., & Kasvar, K.K. (2018, April). Categorization of potential project cost overrun factors in construction industry. In *IOP Conference Series: Earth and Environmental Science* (Vol. 140, No. 1, p. 012098). IOP Publishing.
- Kong, S.M., Oh, D.W., Lee, S.Y., Jung, H.S., & Lee, Y.J. (2021). Analysis of reinforced retaining wall failure based on reinforcement length. *International Journal of Geo-Engineering*, 12, 1-14.
- Koopialipoor, M., Murlidhar, B.R., Hedayat, A., Armaghani, D.J., Gordan, B., & Mohamad, E.T. (2020). The use of new intelligent techniques in designing retaining walls. *Engineering with Computers*, 36, 283-294.
- Liu, Z., He, F., Huang, T.Q., & Jiang, M.D. (2019). Additional earth pressure of retaining wall caused by vehicle load. *Journal of Highway and Transportation Research and Development (English edition)*, 13(1), 16-23.
- Perozzi, D., & Puzrin, A. (2023). *Failure Behaviour of Cantilever Retaining Walls-Soil-Retaining Wall Interaction* (Vol. 715). ETH Zurich.
- Ranjbar Karkanaki, A., Ganjian, N., & Askari, F. (2017). Stability analysis and design of cantilever retaining walls with regard to possible failure mechanisms: an upper bound limit analysis approach. *Geotechnical and Geological Engineering*, 35, 1079-1092.
- Sharma, A., Mohana, R., Kukkar, A., Chodha, V., & Bansal, P. (2023). An Ensemble Learning Based Framework for Smart Landslide Detection, Monitoring, Prediction and Warning in IoT-Cloud Environment.
- Sharma, C., & Baradiya, V. (2014). Evaluation of the effect of lateral soil pressure on cantilever retaining wall with soil type variation. *IOSR Journal of Mechanical and Civil Engineering (IOSR-JMCE)*, 11(2), 36-42.
- Slope Engineering Branch, Jabatan Kerja Raya Malaysia (JKR). (2010). *Guidelines For Slope Design*. http://epsmg.jkr.gov.my/images/e/ee/Design_Guideline.pdf
- Trimble. (2021). Tekla Tedds 2021 user guide. https://support.tekla.com/dist/sxf/document/tekla-tedds-2021-user-guide_0.pdf

- Wahab, F. (2022, May 22). Ikram to investigate retaining wall failure in collapse of Taman Pertama house. *The Star*. <https://www.thestar.com.my/metro/metro-news/2022/05/24/ikram-to-investigate-retaining-wall-failure-in-collapse-of-taman-pertama-house>
- Wang, Z. (2023). *The Impact of Rainfall on Landslide Dynamics: Quantitative Analysis on Mountainous Area in Northern Italy Using Machine Learning Assisted Approaches* (Master's thesis, Duke University).
- Yoo, C., & Jung, H.Y. (2006). Case history of geosynthetic reinforced segmental retaining wall failure. *Journal of Geotechnical and Geoenvironmental Engineering*, 132(12), 1538-1548.